We are IntechOpen,
the world's leading publisher of
Open Access books
Built by scientists, for scientists

6,900
Open access books available

185,000
International authors and editors

200M
Downloads

154
Countries delivered to

Our authors are among the

TOP 1%
most cited scientists

12.2%
Contributors from top 500 universities

CLARIVATE ANALYTICS
BOOK CITATION INDEX
INDEXED

WEB OF SCIENCE™

Selection of our books indexed in the Book Citation Index
in Web of Science™ Core Collection (BKCI)

Interested in publishing with us?
Contact book.department@intechopen.com

Numbers displayed above are based on latest data collected.
For more information visit www.intechopen.com

Vibration Source Contribution Evaluation of a Thin Shell Structure Based on ICA

Wei Cheng[1,2], Zhousuo Zhang[1,*] and Zhengjia He[1]
[1]State Key Laboratory for Manufacturing Systems Engineering, Xi'an,
[2]Department of Mechanical Engineering, University of Michigan, Ann Arbor,
[1]PR China
[2]USA

1. Introduction

As submarines navigate underwater, it is difficult for satellites, anti-submarine aircrafts and warships to detect them. However, the radiated noises produced by the equipment of submarines pose a serious threat to the concealment, and directly influence the operational performance even survivability. Therefore, the reduction and control of vibration and noise is an important work to improve the survival capability and operational performance. As the influences of structural transmission, some components of vibration sources will be changed as they go through mechanical structures, which means the measured vibration signals on the shell are the mixed signals of all the sources. Therefore, it is a challenge but important work to effectively identify the sources and evaluate the source contributions.

The radiated noise of submarines is mainly produced by the diesel engines, and it transmits from the engine bases to the shell according to the hull. One basic method to reduce the radiated noise is based on improving the hull structure to reduce vibration transmission. In the past decades, much research work is devoted to vibration transmission characteristic analysis of different structures, such as beams (Lee et al., 2007), girders (Senjanovic et al., 2009), rafts (Niu et al., 2005), casings (Otrin et al., 2005), panels (Lee et al., 2009), plates (Xie et al., 2007; Bonfiglio et al., 2007) and shells (Efimtsov & Lazarev, 2009). Some studies dedicated to the responses of whole ship hull, such as free vibration analysis of thin shell (Lee, 2006), insertion loss prediction of floating floors (Cha & Chun, 2008) and structural responses of ship hull (Iijima et al., 2008). Another method based on the active control over vibration and noise is also deeply studied in recent years, such as controlling high frequencies of vibration signals by structure modification (Tian et al., 2009), active vibration control using delayed position feedback method (Jnifene, 2007), high frequency spatial vibration control for complex structures (Barrault et al., 2008), and active vibration isolation of floating raft system (Niu, et al., 2005). However, all these techniques are static analysis method, and the radiated noise can be reduced limitedly as the strength requirements of hulls and indispensability of diesel engines.

Aiming at the active control over vibration and noise, a novel approach based on independent component analysis (ICA) is proposed in this paper, which identifies the vibration sources

---

*Corresponding author

from the mixed signals, and quantitatively evaluates the source contributions. Firstly the vibration signals at the different positions are measured, and the radiated noise is evaluated according to the signal energy. Secondly the signals which radiate the noise significantly are selected as the mixed signals, and the source signals contained in the mixed signals are extracted by an improved ICA method. Thirdly, the vibration signals on the engine bases are measured as the source signals, and the vibration sources are identified according to correlation analysis. Lastly, the contributions of each source are quantitatively calculated according to the mixing mode of the independent components. Therefore, the vibration sources which have big contributions can be online identified and controlled if necessary, which provides a novel approach for active control over the vibration and noise.

Compared with other signal processing method, the independent component analysis can reveal the basic sources contained in the mixed signals. ICA is firstly proposed (Jutten & Herault, 1991) and applied in blind source separation (Comon, 1994). A well known ICA algorithm called fixed-point algorithm based on fourth order cumulant is proposed (Hyvarinen & Oja, 1997), and latter fast fixed-point algorithm based on negentropy is proposed (Hyvarinen, 1999), and then is further improved (Hyvarinen, et al., 2001). Currently, ICA is widely used in image feature extraction and recognition (Hu, 2008; Correa et al., 2007), biological signal analysis and feature extraction (Ye et al., 2008; Xie et al., 2008), fault feature extraction (Zuo et al., 2005), astronomical data analysis (Moussaoui et al., 2008), and data compression (Kwak et al., 2008). However, as a statistical signal processing method, a major problem of ICA is that the reliability of the estimated independent components is not known, and the separated components may be different in the repeatedly calculations. Therefore, the independent components are difficult to be explained. A good way to solve this problem is introduced according to clustering evaluation, and the stability of the separated components can be significantly enhanced.

This paper is organized as follows. In section 1, the motivation and research status are introduced. In section 2, the basic theory of ICA is introduced. In section 3, the quantitative calculation of source contributions method based on the enhanced ICA algorithm is proposed. In section 4, the stability of the enhanced ICA algorithm is validated by a comparative numeric study. In section 5, the proposed method is applied to quantitatively calculate the source contributions of a thin shell structure. In section 6, we give the conclusions and discussions.

2. Independent component analysis

2.1 Basic theory of BSS and ICA

Assume that n sources $S = [s_1, s_2, ..., s_n]^T$ exist at the same time, and m mixed signals $X = [x_1, x_2, ..., x_m]^T$ which are composed by these sources are obtained in different places. And thus each mixed signals can be described as:

$$x_i = \sum_{i=1}^{n} a_{ij} s_j + n_i \quad i = 1, 2, ..., m, \quad j = 1, ..., n \tag{1}$$

Where x_i is the ith mixed signal observed in the position i, s_j is the jth source signal, a_{ij} is the mixing coefficient, and n_i is the noise of ith mixed signal.
The mixed signal can be also described as:

$$X = AS + N \tag{2}$$

Where A is the mixing matrix, and N is the noise matrix.

Blind source separation (BSS) can be described as follows: in the condition that the mixing matrix and source signals are unknown, BSS obtains the estimates of sources $Y = [y_1, y_2, ..., y_n]^T$ according to separating matrix W and mixed signals. That is

$$Y = WX = WAS = GS \tag{3}$$

Where G is a global matrix.

2.2 Assumptions of independent component analysis

As a result of unknown source signals and mixing mode, information that can be used by ICA is only the mixed signals observed by the sensors, which will give multiple solutions of the problem. Therefore, some assumptions are necessary to get a definite solution:

1. Each source signal $s_j (j = 1, ..., n)$ is zero mean and real random variable, and all the source signals are mutually statistic independent at any time.

$$p_s(s) = \prod_{j=1}^{n} p_j(s_j) \tag{4}$$

Where $p_s(s)$ is the probability density of source signals S, and $p_j(s_j)$ is the probability density of source signal s_j.

2. The number of sources are less than the number of mixed signals($n \leq m$).
3. Only one source is allowed to have a guassian distribution.

2.3 Separating criterion based on negentropy

Assume that one random variable is composed of some independent variables according to superposition. According to the central limit theorem, the superposed variable will tend to a Gaussian distribution if the independent variables have the same limited means and variances. Therefore, Gaussian feature are always used to determine whether the separating components are independent or not.

Assume that a source signal s has a probability density $p(s)$, and its negentropy is defined as follow equation:

$$Ng(s) = H(s_{Gauss}) - H(s) \tag{5}$$

Where s_{gauss} is a signal of Gaussian distribution and has the same variance with s. $H(\bullet)$ is the information entropy of a signal.

$$H(s) = -\int p(s) \lg p(s) ds \tag{6}$$

As the probability density distribution function is unknown, the independence of each separated signal is commonly measured by an approximate equation

$$Ng(s) \propto [E\{G(s)\} - E\{G(s_{gauss})\}]^2 \tag{7}$$

Where $E(\bullet)$ is a mean function, and $G(\bullet)$ is a nonlinear function. The commonly used $G(\bullet)$ are logarithmic function and exponential function

$$G(u) = \frac{1}{a} \lg \cosh(au) \tag{8}$$

$$G(u) = -\exp(-u^2 / 2) \tag{9}$$

Where $1 \le a \le 2$.

The independent component analysis method based on negentropy has obvious advantages, such as simple concept, fast computing speed and good stability. It can be also used to determine whether the separating process should be stopped or not according to non-gaussian feature of the separated components.

2.4 Framework of fast fixed-point algorithm

Fast fixed-point algorithm based on the negentropy criterion is a typical independent component analysis algorithm. Its calculation process includes two steps: signal preprocessing and extracting components one by one. The projection pursuit method is applied to extracting the independent components, and the framework of fast fixed-point algorithm can be described as eight steps:

1. Mean and whiten the mixed signals X , remove the redundant information, and thus obtain the preprocessed signals Z .
2. Set the number p of independent component esxtracted for each time.
3. Set the initial iteration value $u_p(0)$, and let $\left\| u_p(0) \right\|_2 = 1$.
4. Iterative calculation

$$u_p(k+1) = E[zg(u_p^T(k)z)] - E[g'(u_p^T(k)z)]u_p(k) \tag{10}$$

where g is the differential of G
5. Orthogonal calculation

$$u_p(k+1) = u_p(k+1) - \sum_{j=1}^{p-1} <u_p(k+1), u_j> u_j \tag{11}$$

6. Normalizing calculation

$$u_p(k+1) \leftarrow \frac{u_p(k+1)}{\left\| u_p(k+1) \right\|_2} \tag{12}$$

7. Determine whether u_p is convergent. If not, return to step (4).
8. Repeat step (3), and else stop calculation.

3. Quantitatively calculate source contributions

To quantitatively calculate source contributions, a novel method based on an enhanced ICA algorithm and priori information is proposed in this paper. The enhanced ICA algorithm

extracts independent components by running a single ICA algorithm for many times, and selects the optimal components as the optimal independent components according to clustering analysis (Hamberg & Hyvarinen, 2003; Hyvarinen et al., 2004). The proposed method separates mixed signals into independent components by the enhanced ICA algorithm, and calculates source contributions according to the mixing matrix. Priori information was employed to further enhance the separating performance, because priori information is proved to be able to weaken the uncertainty of problems (Ma, et al., 2006).

3.1 Framework of fast fixed-point algorithm

For linear superposition model, fast fixed-point algorithm has good separating performance. However, most algorithms based on ICA are stochastic, and their results may be different in repeatedly calculations, so the outputs of a single run can not be trusted (Hamberg & Hyvarinen, 2003; Hyvarinen et al., 2004). One reason for this problem is that engineering data is not strictly complied with the blind source separation model, and the actual calculation algorithm may converge to local minima rather than the overall minimum value. The other reason is the statistical error of estimated components which is caused by the finite sample size.

To enhance the stability of ICA, an enhanced ICA algorithm is constructed based on clustering evaluation. At first the independent components (ICs) are extracted according to a single ICA algorithm for many times, and then the reliability of each IC is estimated by clustering analysis and the optimal Ics are selected as the best solutions. Basic framework of the enhanced ICA algorithm is as follows:

1. Parameters of a single algorithm are set, such as orthogonalization approach and the nonlinearity function.
2. The single ICA algorithm is executed for certain times with different initial values to produce more results in the different condition.
3. All the ICs are clustered according to their mutual similarities, and then these ICs are divided into several clusters. According to the average-linkage clustering criterion, the clustering center which has the largest relevances with other components is selected as the optimal results.

Assume that the mutual correlation coefficient between estimated components y_i and y_j is ρ_{ij}, and the cluster validity index I_q can be defined as follows:

$$I_q(k) = \frac{1}{|C_k|^2} \sum_{i,j \in C_k} \rho_{ij} - \frac{1}{|C_k||C_{-k}|} \sum_{i \in C_k} \sum_{j \in C_{-k}} \rho_{ij} \tag{13}$$

where C is all the IC set, C_k is the IC set in the kth cluster, C_{-k} is its complementary set, and $|C_k|$ is the size of the kth cluster.

By the clustering evaluation method, the ICs produced by the enhanced ICA algorithm are clustered into different clusters, and the separating performance can be indicated by the tightness of ICs. The more tightness they are, the better the separating performance will be. After clustering, the cluster center is selected as the optimal ICs.

3.2 Priori information

In the applications, some mixed signals do not follow the linear superposition model. Therefore, priori information should be used to weaken the uncertain problems. For sources $S = [s_1, s_2]^T$, it can be inferred that the joint distribution $p_{s_1,s_2}(s_1, s_2)$ of the two source signals must be included in a rectangle as

$$p_{s_1,s_2}(s_1,s_2) = p_{s_1}(s_1)p_{s_2}(s_2) \tag{14}$$

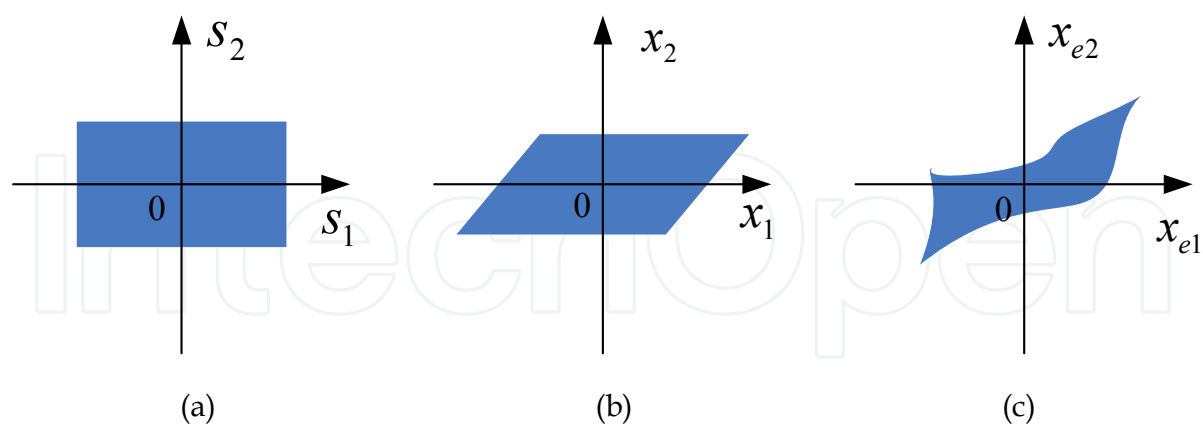(a)   (b)   (c)

Fig. 1. Joint distributions of different signals

The joint distribution of S is shown in Fig. 1(a). Mixed signals are obtained according to S and mixing matrix A, which can be shown as

$$X = AS = [x_1, x_2]^T \tag{15}$$

The joint distribution of X is shown in Fig. 1(b). Nonlinear mixed signals $X_e = [x_{e1}, x_{e2}]^T$ are obtained by nonlinear mixing mode, and their joint distribution is shown in Fig. 1(c).
Theorem 1: for transformation

$$\begin{cases} p_1 = h_1(e_1) \\ p_2 = h_2(e_2) \end{cases} \tag{16}$$

Where h_1 and h_2 is an analytic function.
If the parallelogram border on the plane (e_1, e_2) is transformed into the plane (p_1, p_2), and these parallelogram borders are not parallel to the related coordinate axis, there have real constants $a_1 \cdot a_2 \cdot b_1$ and b_2

$$\begin{cases} h_1(u) = a_1u + b_1 \\ h_2(u) = a_2u + b_2 \end{cases} \tag{17}$$

The theorem 1 provides a transmission from nonlinear mixed signals to linear mixed signals based on priori information, and this method does not need the assumption of independence. The limited border of source signals provides additional information, which can optimize the nonlinear parts of the mixed signals. Therefore, the separating performance of the proposed method is further enhanced.

3.3 Quantitative evaluation of source contributions
From the definition of whitening, the covariance matrix R_{xx} can be described as

$$R_{xx} = E[xx^T] = E[Qxx^TQ^T] = QR_{xx}Q^T = I_n \tag{18}$$

Where Q is a whitening matrix, and I_n is a unit covariance matrix. From the equation (18), it can be seen that the mixed signals $X = [x_1, x_2, ..., x_n]^T$ are transformed into unrelated signals $Z = [z_1, z_2, ..., z_n]^T$ by whitening.

According to the definition of orthogonal transformation, there exists follow equation

$$UU^T = U^T U = I_n \tag{19}$$

$$Y = UZ \tag{20}$$

$Y = [y_1, y_2, ..., y_n]^T$ are independent components with unit variances. From the mathematical model of ICA, mixed signals X can be obtained by Y.

$$X = AS = AG^{-1}Y = \hat{A}Y \tag{21}$$

Each components of X are composed by all the components of Y according to the mixing matrix $\hat{A}$. Each combination coefficients of the mixing matrix $\hat{A}$ reveal the contribution of the related independent components. Therefore, the quantitative calculation of source contribution problem in essential is how to obtain the mixing matrix $\hat{A}$ effectively.

4. Simulation experiment analysis

4.1 Validation of separating performance

When the rotational parts, such as gears and rolling bearings occur faults (teeth broken, peeling or rubbing), the vibration signals measured on the shell will be frequency and amplitude modulated (He et al., 2001), and thus the source signals(teeth broken, peeling or rubbing) can not be well revealed just by the measured signals. As the composite faults occur, the vibration signal will be coupled together, and thus it is difficult to reveal the conditions of each parts. Therefore, some vibration signals of typical fault features are selected to test the separating performance of different methods.

Four source signals are selected: $s_1(t)$ is a white noise signal, $s_2(t)$ is a frequency modulated signal, $s_3(t)$ is an amplitude modulated signal, and $s_4(t)$ is a both amplitude and frequency modulated signal. The data length of t is 1000 and the step is 1. The generating functions of sources and mixing matrix are listed as follows.

$$S(t) = \begin{bmatrix} s_1(t) \\ s_2(t) \\ s_3(t) \\ s_4(t) \end{bmatrix} = \begin{bmatrix} n(t) \\ \sin(0.2 \times t) \times \cos(15 \times t) + \sin(2 \times t) \\ \sin(0.3 \times t) \times \sin(5 \times t + \sin(t)) \\ \sin(0.3 \times t \times \sin(0.5 \times t)) \end{bmatrix}$$

$$A = \begin{bmatrix} 0.63 & 0.77 & 0.54 & 0.65 \\ 0.94 & 0.72 & 0.78 & 0.83 \\ 0.88 & 0.93 & 0.84 & 0.32 \\ 0.98 & 0.62 & 0.54 & 0.95 \end{bmatrix} \tag{22}$$
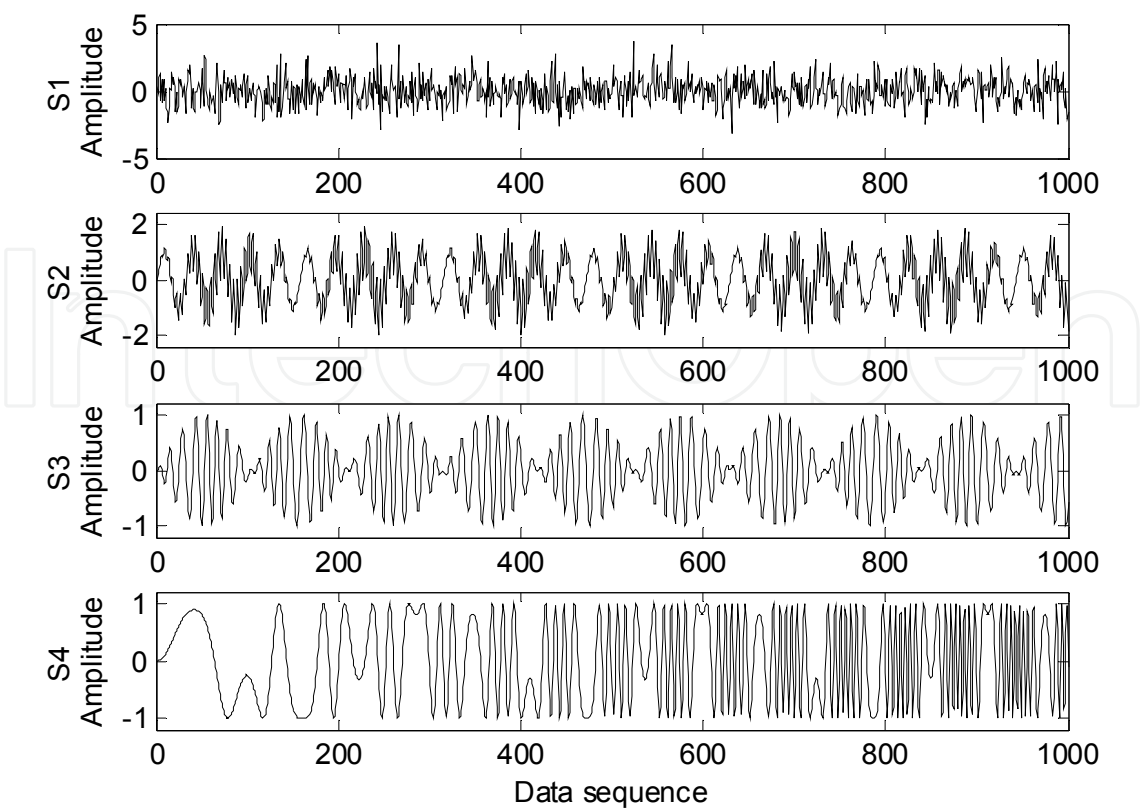
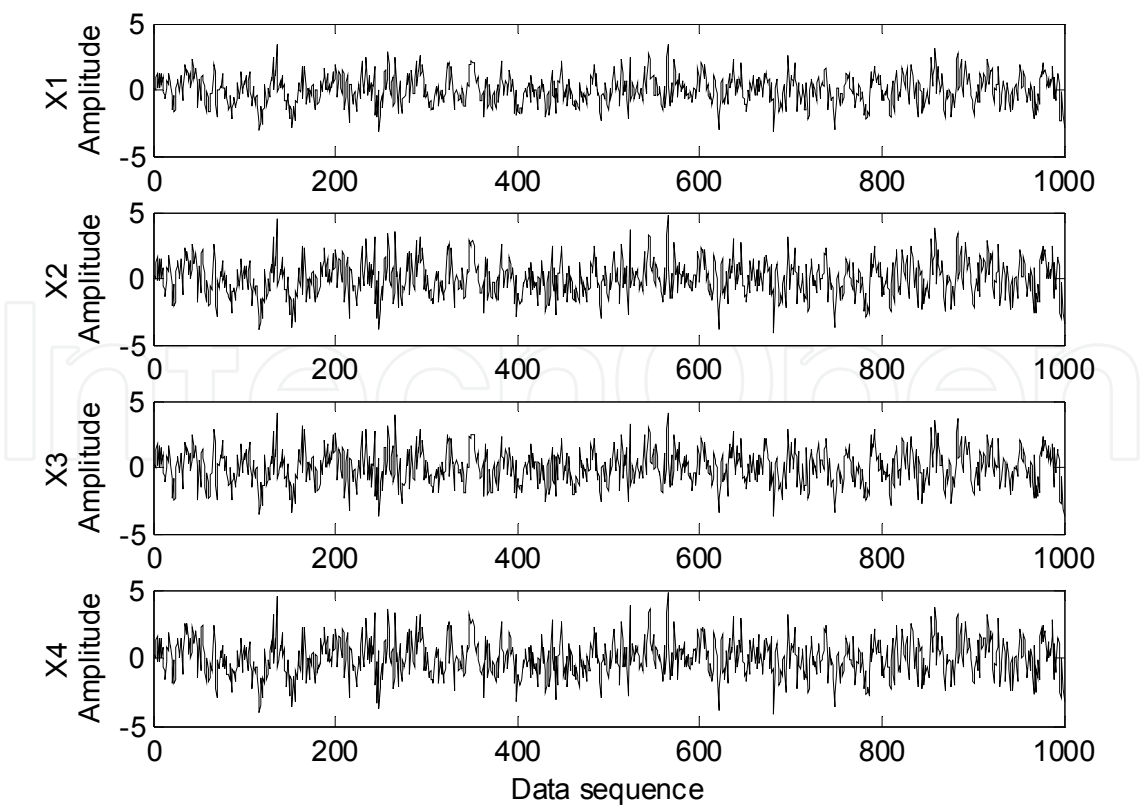Fig. 2. Waveforms of the source signals

Fig. 3. Waveforms of the mixed signals

Waveforms of the sources are shown in Fig.2, which indicates that each source is of obviously different waveform features. The mixed signals are composed of four sources by mixing matrix with linear superposition, and the mixed signals are shown in Fig. 3.
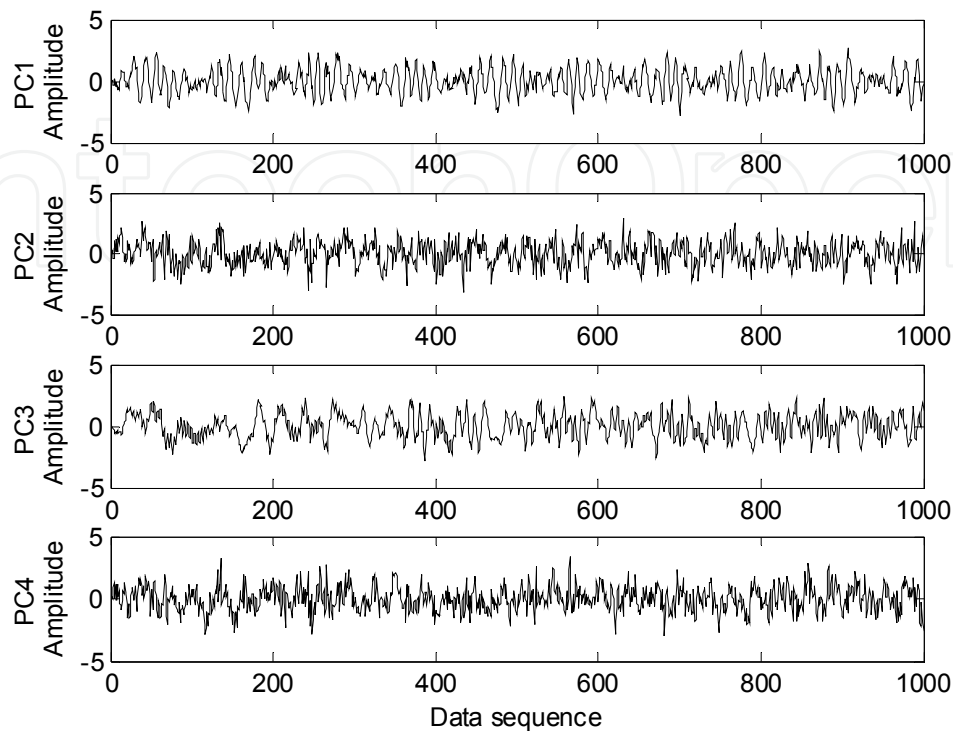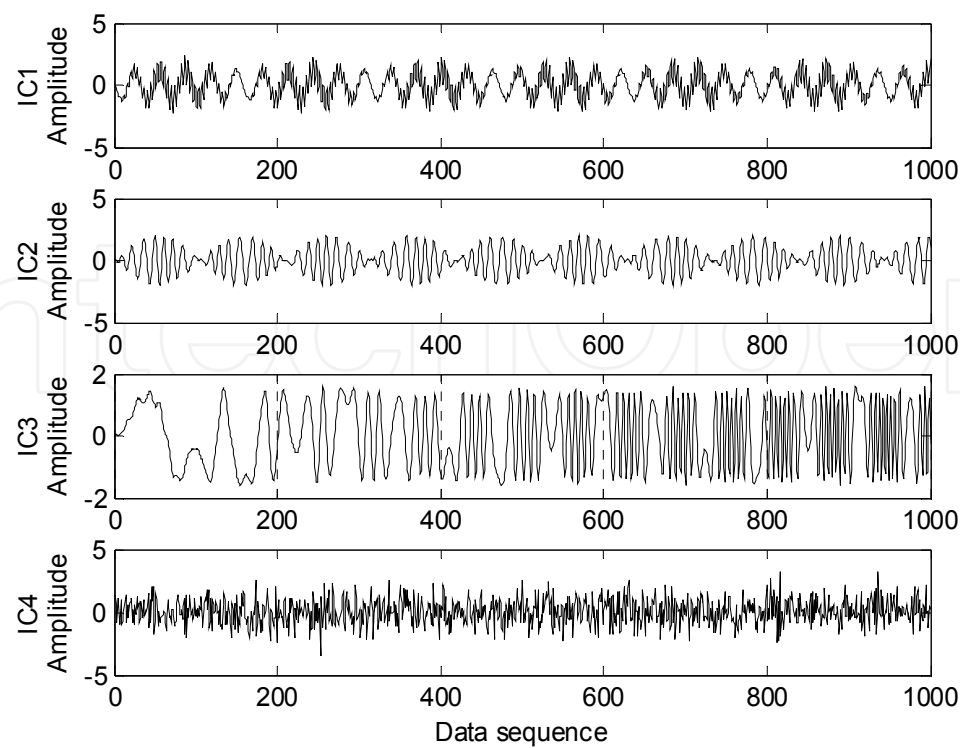

Fig. 4. Waveforms of principal components

Fig. 5. Waveforms of independent components by fast fixed-point algorithm

Three different BSS methods are applied to separate the mixed signals, including principal component analysis based on second-order cumulant, fast fixed-point algorithm based on negentropy, and the enhanced ICA algorithm based on clustering optimization. The waveforms of the separated components are shown in Fig. 4 - Fig. 6 respectively.
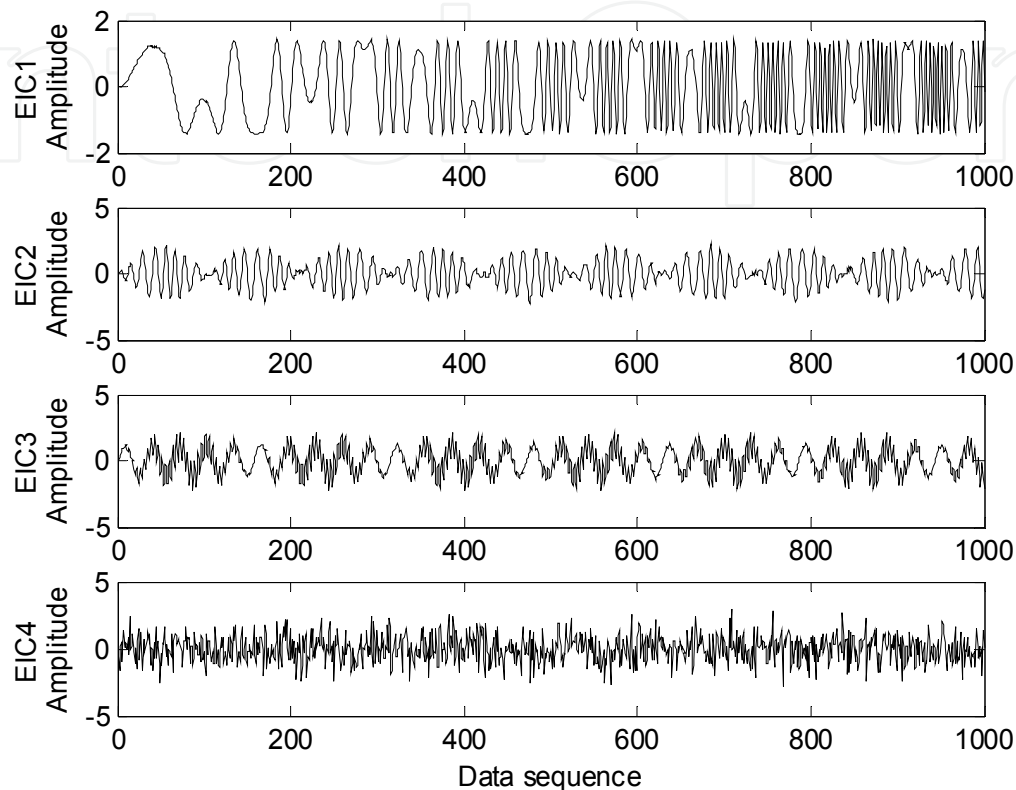
Fig. 6. Waveforms of the separated components by the enhanced ICA

From Fig. 4 to Fig. 6, it can be clearly seen that principal component analysis only separate s_3, and the other sources are not well separated. The independent components separated by the other two algorithms are obvious, and the waveform information of the sources is well separated. Correlation analysis is employed to quantitatively validate the separating performance, and the correlation coefficient ρ_{sy} is defined as follows.

$$\rho_{sy} = \frac{\sum\limits_{k=1}^{n} s(k)y(k)}{\sqrt{\sum\limits_{k=1}^{n} s^2(k) \sum\limits_{k=1}^{n} y^2(k)}} \tag{23}$$

Where $s(k)$ is the source signal, $y(k)$ is the independent component, and k is the data sequence.

In the numeric studies, the correlation matrices Ω_{sy} between the separated components and the sources are listed as follows:

1. Ω_{sy} of principal component analysis

$$\Omega_{sy} = \begin{bmatrix} 0.2684 & 0.2317 & \underline{0.8932} & 0.1903 \\ 0.6154 & \underline{0.5829} & 0.1837 & 0.4735 \\ 0.1280 & 0.5709 & 0.3356 & \underline{0.7673} \\ \underline{0.7299} & 0.5298 & 0.2363 & 0.3942 \end{bmatrix}$$

2. Ω_{sy} of the fast fixed-point algorithm

$$\Omega_{sy} = \begin{bmatrix} 0.0687 & \underline{0.9996} & 0.0092 & 0.0429 \\ 0.0835 & 0.0120 & \underline{0.9988} & 0.1561 \\ 0.0984 & 0.0404 & 0.1527 & \underline{0.9952} \\ \underline{0.9986} & 0.0689 & 0.0793 & 0.0988 \end{bmatrix}$$

3. Ω_{sy} of the enhanced ICA algorithm

$$\rho_{sy} = \begin{bmatrix} 0.0873 & 0.0402 & 0.1532 & \underline{0.9997} \\ 0.0833 & 0.0185 & \underline{0.9913} & 0.1535 \\ 0.0647 & \underline{0.9980} & 0.0407 & 0.0418 \\ \underline{0.9859} & 0.1245 & 0.1267 & 0.0809 \end{bmatrix}$$

Comparing the three Ω_{sy} by different methods, the correlation coefficients between each components and related source signals of fast fixed-point algorithm and the enhanced ICA algorithm are more than 0.98, which means waveform information implied in the mixed signals is well extracted. Therefore, these two algorithms have good separating performance. However, the correlation coefficient between the second component and s_2 is only 0.58, but the other correlation coefficients are even up to 0.61, which means the source information is not well separated. Therefore, principal component analysis fails to separate the sources effectively in this case.

4.2 Stability validation of the enhanced ICA algorithm

As a statistical signal processing method, fast fixed-point algorithm may produce different results in repeated executions, and thus the separated components will be unreliable. To illustrate this problem clearly, another case is given in this section.

The source signals are: s_5 is a white noise signal, s_6 is a sinusoidal signal, s_7 is a triangle wave signal, and s_8 is a square wave signal. The generating function of sources and the mixing matrix A are as follows:

$$S(t) = \begin{bmatrix} s_5(t) \\ s_6(t) \\ s_7(t) \\ s_8(t) \end{bmatrix} = \begin{bmatrix} n(t) \\ sin(0.4 \times \pi \times t) \\ sawtooth(0.5 \times \pi \times t, 0.5) \\ square(0.6 \times \pi \times t, 50) \end{bmatrix} \qquad A = \begin{bmatrix} 0.65 & 0.75 & 0.65 & 0.60 \\ 0.95 & 0.70 & 0.75 & 0.85 \\ 0.88 & 0.90 & 0.80 & 0.32 \\ 0.90 & 0.40 & 0.42 & 0.95 \end{bmatrix} \qquad (24)$$

The waveforms of source signals and the mixed signals are shown in Fig. 7 and Fig. 8 respectively. The fast fixed-point algorithm is repeatedly executed for more than 30 times, and more than 60% of the results show that the ICs are accurate. However, the other 40% of

the results are different from the source signals obviously. One of the inaccurate results is shown in Fig. 9, which indicates that the source information is not well separated.
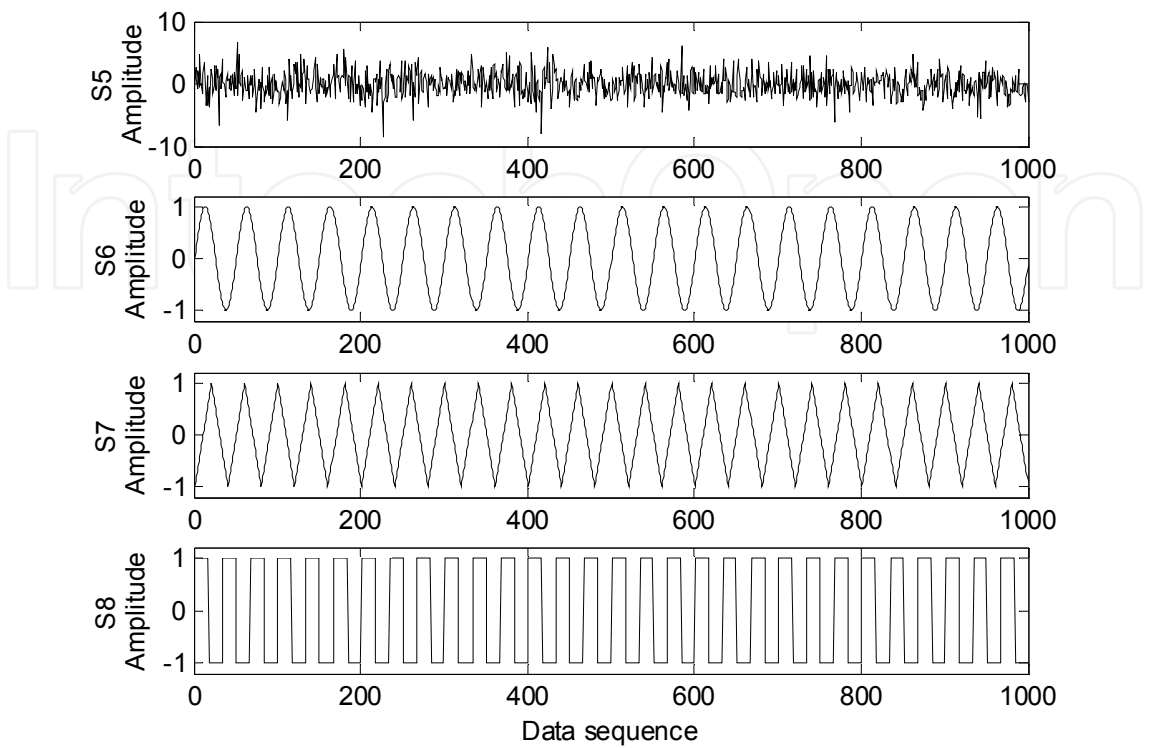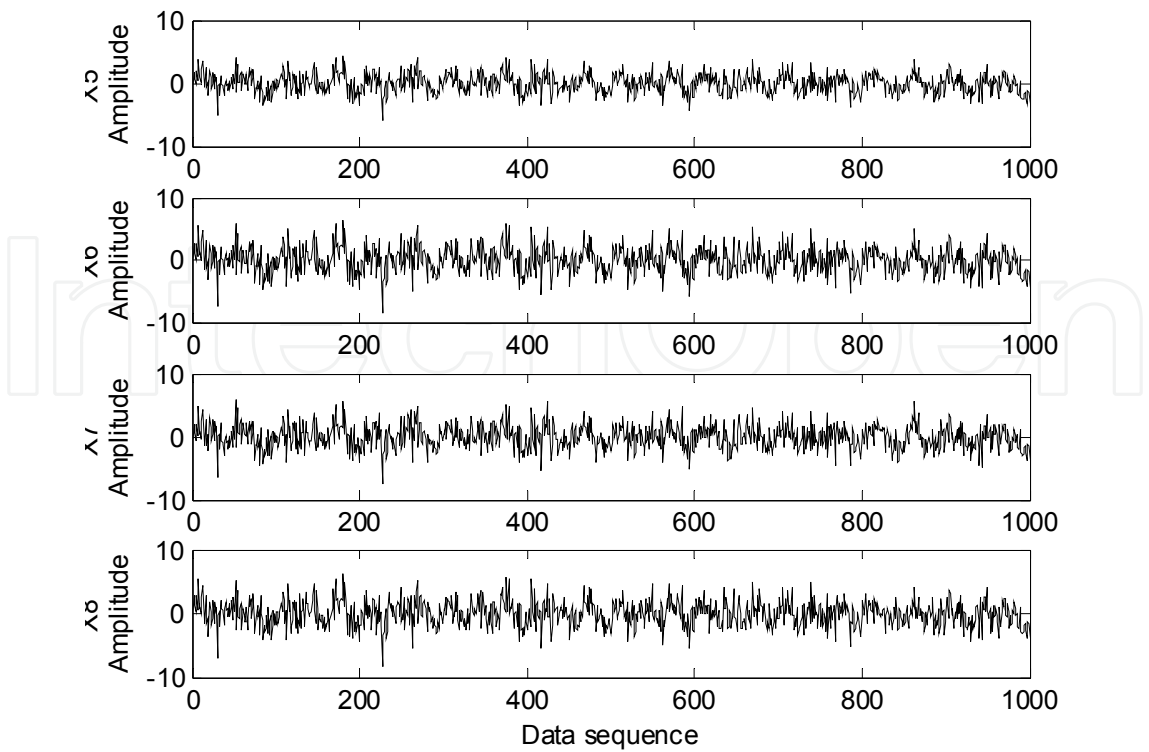
Fig. 7. Waveforms of the source signals

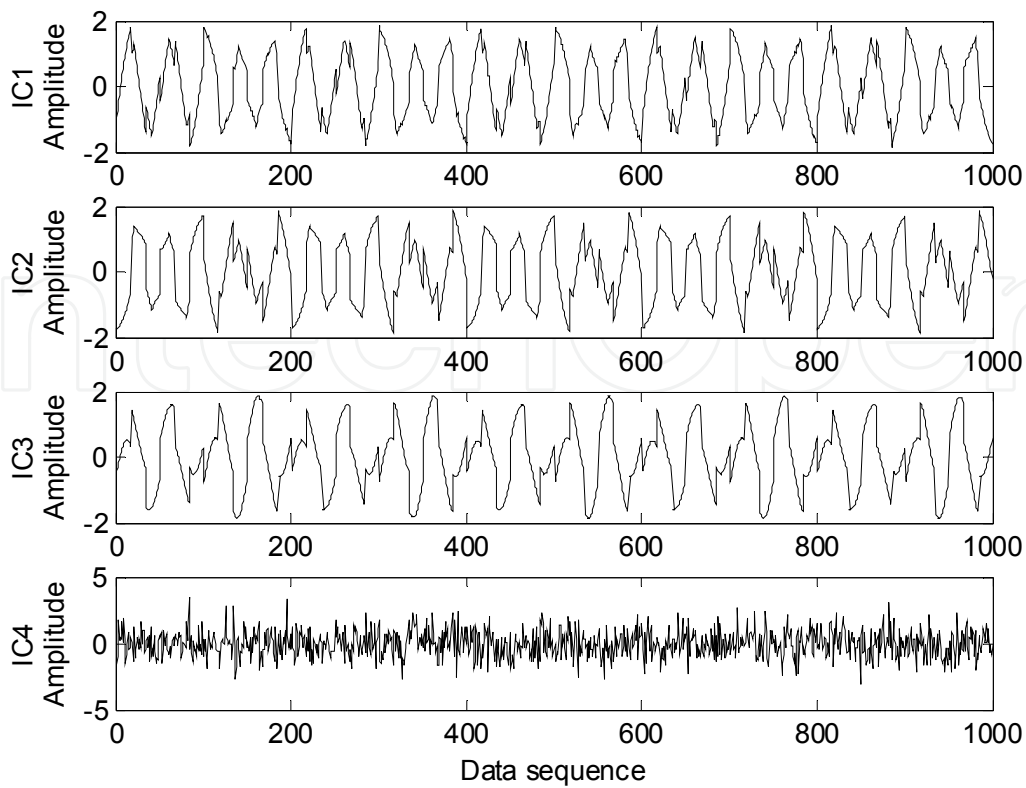Fig. 8. Waveforms of the mixed signals

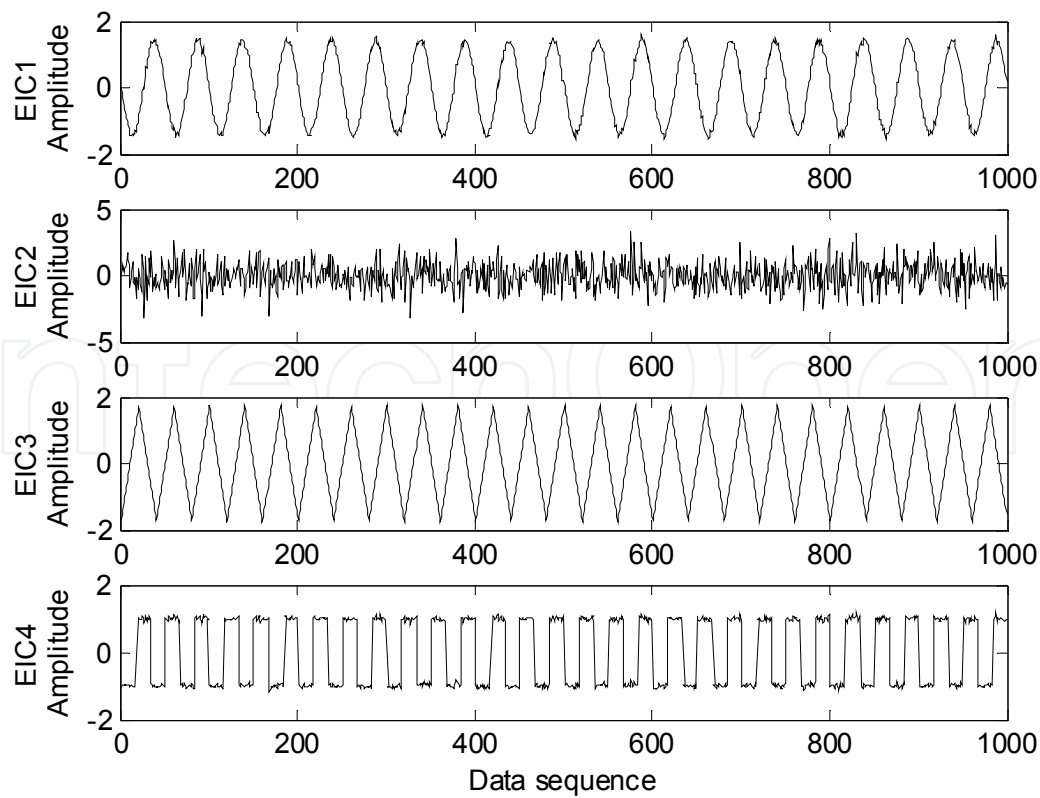Fig. 9. Waveforms of one inaccurate separation by fast fixed-point algorithm

Fig. 10. Waveforms of separated components by the enhanced ICA algorithm

To enhance the stability of traditional ICA, the enhanced ICA algorithm is constructed. The enhanced ICA algorithm is repeatedly executed for 20 times, and all the result is stable. The waveforms of the separated components by the enhanced ICA algorithm are shown in Fig. 10, which indicates that the source information is well extracted.

It can be concluded that fast fixed-point algorithm may produce inaccurate components because it is a statistic signal processing method. To enhance the stability, an effective way is to execute the single ICA algorithm for certain times, and evaluate the separated components by clustering analysis. Therefore, the enhanced algorithm based on clustering optimization is of high precision and stability.

4.3 Quantitative evaluation of source contributions

From the basic theory of blind source separation model, it can be explained that some complicate signals are composed of several independent components, and the combination relationship of the independent components reveals their contributions. Therefore, source contributions can be obtained according to the mixing matrix.

We take the case in section 4.1 to show the numeric studies of source contribution evaluation. After the separation, a mixing matrix A' of the independent components for the mixed signals is obtained. As the source signals and the independent components have different scales. We add a factor to let the independent components have the same energy with the related sources, and thus get a modified mixing matrix $\hat{A}$.

$$A = \begin{bmatrix} 0.63 & 0.77 & 0.54 & 0.65 \\ 0.94 & 0.72 & 0.78 & 0.83 \\ 0.88 & 0.93 & 0.84 & 0.32 \\ 0.98 & 0.62 & 0.54 & 0.95 \end{bmatrix} \leftrightarrow \hat{A} = \begin{bmatrix} 0.65 & 0.75 & 0.55 & 0.62 \\ 0.95 & 0.70 & 0.75 & 0.85 \\ 0.88 & 0.90 & 0.80 & 0.32 \\ 0.94 & 0.60 & 0.52 & 0.95 \end{bmatrix}$$

Compared the mixing matrix A with the mixing matrix $\hat{A}$ calculated by the proposed method, the real proportion of each source to x_1 are 0.63, 0.77, 0.54 and 0.65, while the contributions calculated by the proposed method are 0.65, 0.75, 0.55 and 0.62, which means the relative error between the calculated values and the real values is less than 4.6%. The calculated results of source contributions to x_2, x_3 and x_4 are also close to the real values, and the relative errors are all less than 4.8%. Therefore, the comparative results show that it is effective to quantitatively evaluate the source contributions just from the mixed signals.

5. Source contribution evaluation of a thin shell structure

5.1 Introductions of the thin shell structure

In this application, a thin shell structure is set up to validate the effectiveness of the proposed method. Three motors are installed in the thin shell structure to simulate the vibration sources, and blocks are added in each output shaft of the motors to generate eccentric vibration. Magnetic brakes are installed in the output shaft of these motors for a variable load. Rubber springs are applied to support the entire structure, and they can also eliminate the environmental influences. The structural diagram of the thin shell structure is shown in Fig.11, and the photo of the entire system is shown in Fig.12.
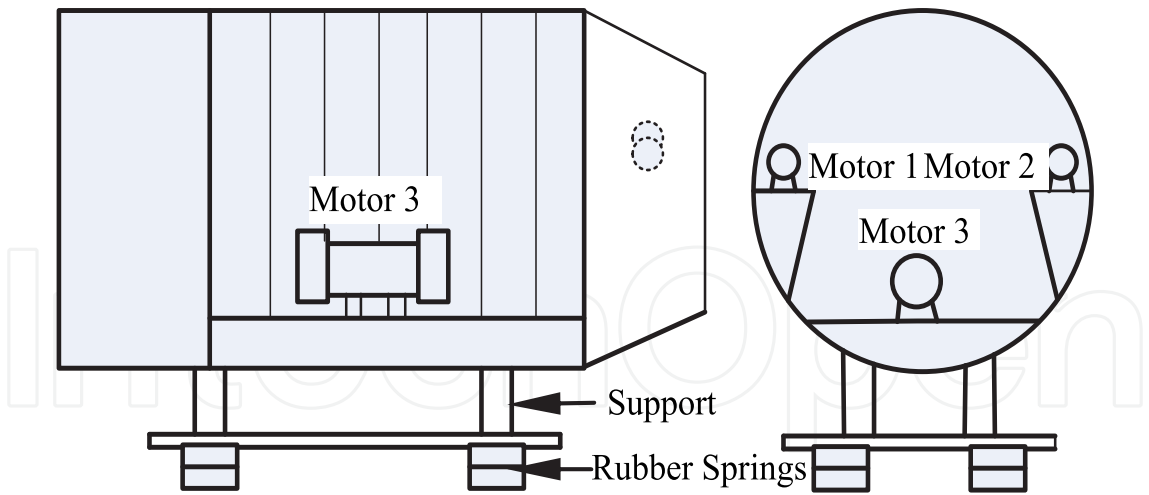
Fig. 11. The structural diagram of the thin shell structure

Fig. 12. The photo of the entire system

Acceleration sensors are used to sample the vibration signals. Three sensors are installed in the bases of each motor to measure the sources, and nine sensors are installed on the left inside shell to measure the mixed signals. In the testing, the sampling frequency is 16384 Hz, the data length is 16384, and the unit of measured signals is g (1.0g=9.8m/s^2). The rotational speeds of motor 1, motor 2, and motor 3 are respectively 1350 rpm, 1470 rpm, and 1230 rpm.

5.2 Blind source separation of the mixed signals

To calculate the source contributions quantitatively, a direct method is to separate the mixed signals and calculate the contributions by the mixing matrix. Three vibration signals on the inside shell are selected as the mixed signals, and their waveforms are shown in Fig. 13. The enhanced ICA algorithm is applied to separate the mixed signals, and three independent components extracted are shown in Fig. 14. Three source signals are measured on the motor

bases, and their waveforms are shown in Fig. 15. From Fig. 15, it can be clearly seen that the waveforms of the independent components are obviously different from the source signals.
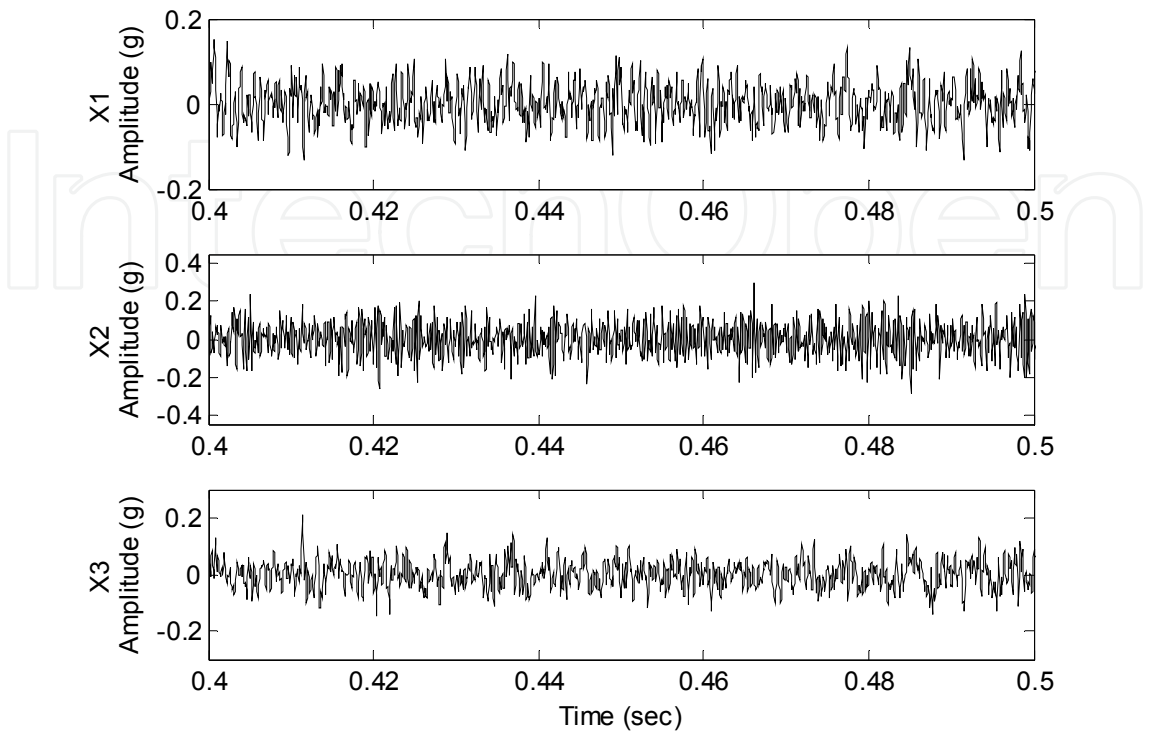

Fig. 13. Waveforms of the mixed signals on the inside shell
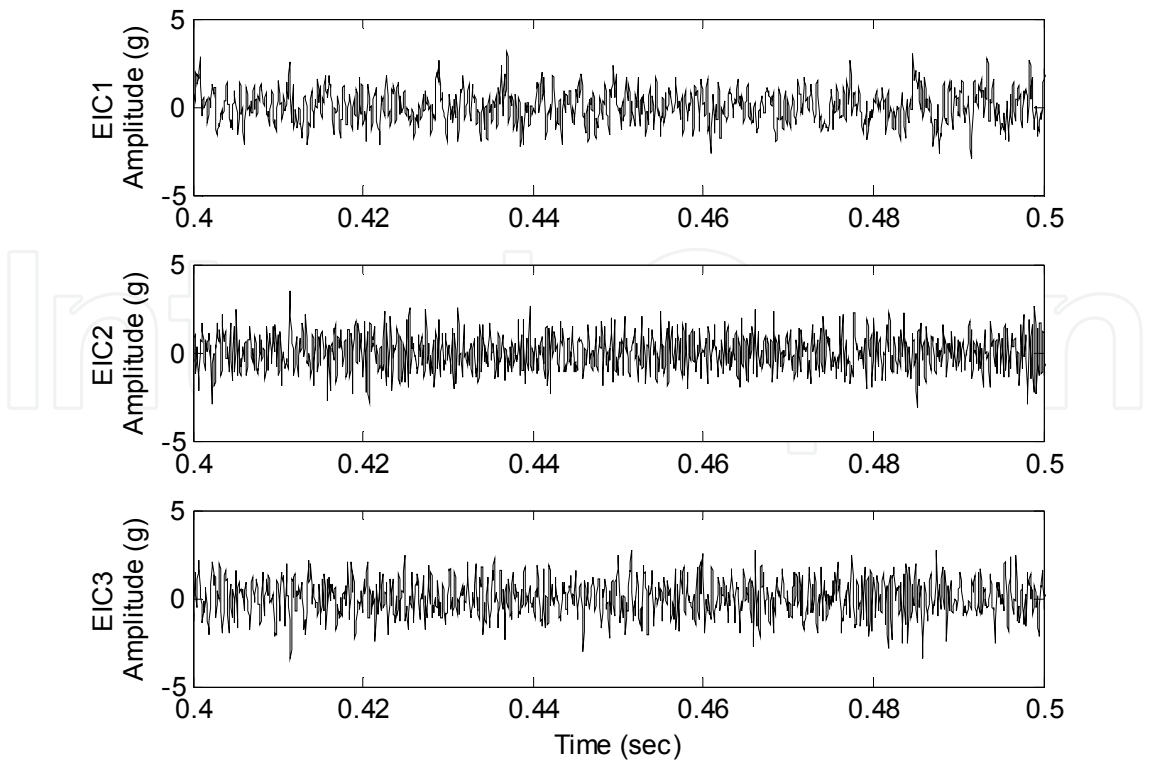

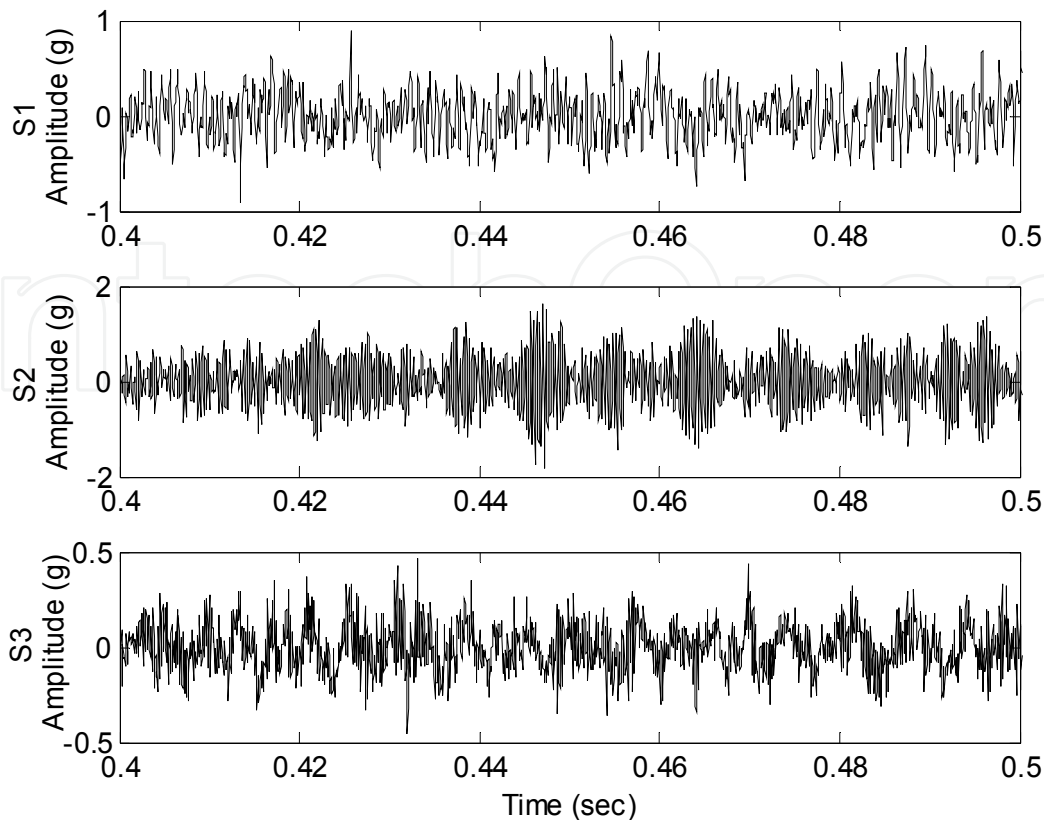Fig. 14. Waveforms of the ICs by the enhanced ICA algorithm

Fig. 15. Waveforms of the source signals from three motor bases

The correlation matrix Ω_{sy} is as follows.

$$\Omega_{sy} = \begin{bmatrix} 0.2955 & 0.2471 & 0.4269 \\ 0.2614 & 0.4235 & 0.1621 \\ 0.3376 & 0.3898 & 0.2217 \end{bmatrix}$$

Ω_{sy} shows that the correlation coefficients between independent components and source signals are relatively small, and the maximum coefficient is only 0.4269, which indicates that the source information is not well separated. Therefore, the separated components extracted cannot be regarded as the sources for calculating source contributions.

5.3 Source contribution evaluation based on priori information

In this application, source signals can be obtained from the motor bases. Source contribution based on priori information is proposed and it can be described as follows: four signals are selected as the mixed signals, one of them is measured inside shell, and the other three signals are measured from the motor bases. The waveforms of the mixed signals are shown in Fig.16. The independent components are extracted by the enhanced ICA algorithm. The optimal independent components are selected by clustering evaluation, and waveforms of the optimal independent components are shown in Fig.17. Obviously three independent components have the similar waveforms with three source signals.

Correlation matrix Ω_{sy} between independent components and source signals are:

$$\Omega_{sy} = \begin{bmatrix} 0.2907 & \underline{0.8903} & 0.0795 \\ \underline{0.8397} & 0.1041 & 0.3083 \\ 0.2717 & 0.1094 & \underline{0.9539} \end{bmatrix}$$

The correlation matrix Ω_{sy} shows that the correlation coefficient between IC 1 and source signal 2 is 0.8397, IC 2 and source signal 1 is 0.8903, and IC 3 and source signal 3 is up to 0.9539, which shows that three source signals are well extracted from the mixed signals. Therefore, with the priori information, the source information can be well separated in the real applications, which means the priori information can further improve the separating performance. After the separation, the mixing matrix is calculated by the enhanced ICA algorithm. The mixing matrix $\hat{A}$ is as follow:

$$\hat{A} = \begin{bmatrix} -0.1299 & -0.0097 & 0.0440 \\ -0.1971 & 0.0358 & 0.1656 \\ 0.1424 & 0.0318 & 0.0708 \\ -0.0313 & -0.1375 & 0.0275 \end{bmatrix}$$
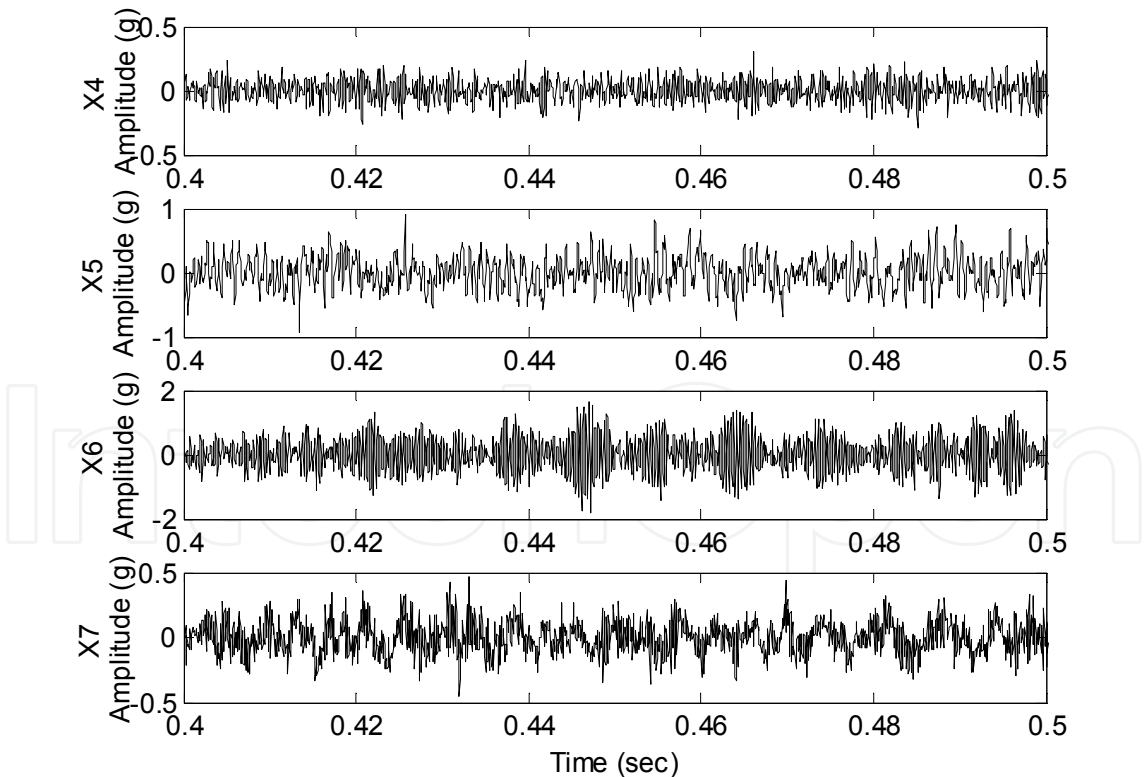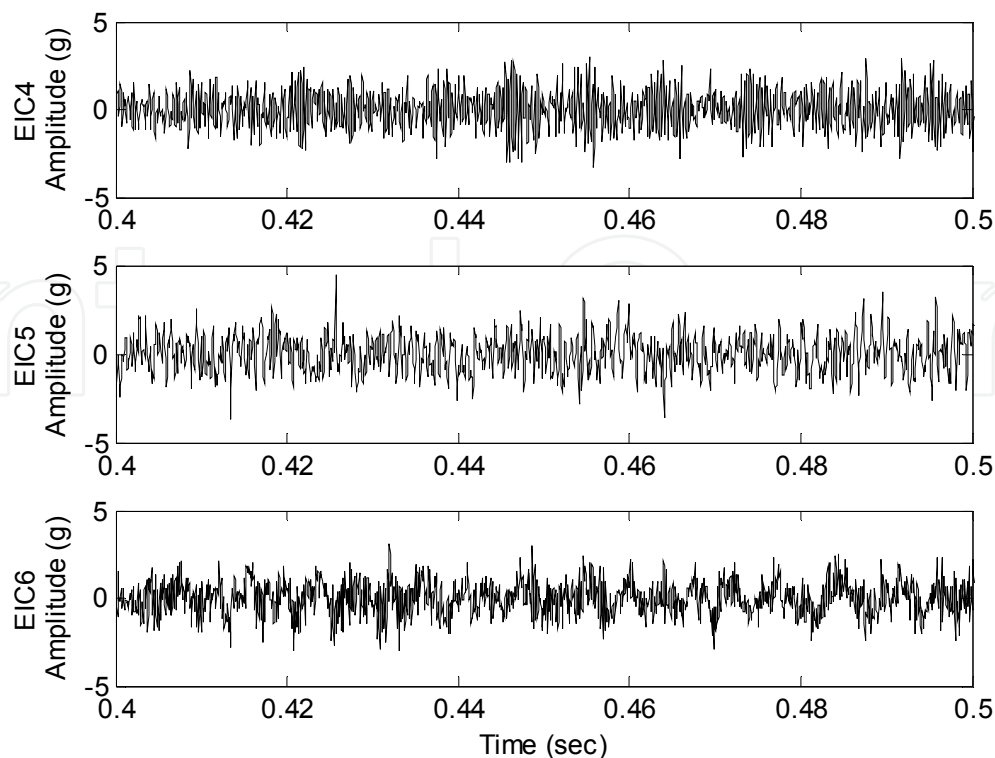

Fig. 16. Waveforms of the mixed signals

Fig. 17. Waveforms of ICs by the enhanced ICA algorithm with priori information

The mixing matrix $\hat{A}$ shows that the mixed signals are composed of three ICs, and their proportional contributions are 0.1299, 0.0097 and 0.0440. The three ICs represent the source signals from three motors, and the percentage contributions of motor 1, motor 2 and motor 3 are 23.97%, 70.75% and 5.280% respectively. The percentage contribution indicates that IC 2 (motor 3) has the largest vibration contribution, which means that mixed signal 1 mainly comes from the motor 3. Therefore, motor 3 should be controlled or the vibration reduction equipments should be adapted in the transmission path to reduce vibration.

Contributions	Motor 1	Motor 2	Motor 3
Measurement	16.79%	5.66%	77.55%
Without priori information	47.19%	11.93%	40.88%
Proposed Method	23.97%	5.28%	70.75%

Table 1. Percentage contributions

In the measuring point on the shell, the real vibration contributions are measured in the condition that only one motor is running at the given speed (motor1 - 1350 rpm, motor2 - 1470 rpm and motor3 - 1230 rpm respectively), and thus the contribution of the related motor to the same location on the shell can be measured one by one. The energy contributions of motor 1, motor 2 and motor 3 are 5.41, 1.82 and 24.98 respectively. The real contributions also show that motor 3 has the largest contribution. This paper also gives the source contributions calculated by the enhanced ICA without priori information. The percentage contributions are listed in Tab .1. Tab. 1 shows that the real contribution of motor 3 is up to 77.55%, which means that motor 3 gives a large vibration contribution to the shell. The contribution of motor 3 calculated by the enhanced ICA method without priori

information is 40.88%, which has a relative error of 36.67%. The relative error of the proposed method is 6.8%, and the other two motor contributions also show that the proposed method has high accuracy. Therefore, it can be concluded that the accuracy of the proposed method has been greatly enhanced by priori information.

5.4 Discussions

1. The key process of quantitative calculation of source contributions is that mixed signals are well separated. Principal component analysis in the simulation does not give a satisfied result, and fast fixed point algorithm has good separating performance for linear superposition but it is not stable for repeatedly calculation. The enhanced ICA algorithm executes the single ICA algorithm for several times, and selects the optimal ICs by clustering analysis. Therefore, separating performance and reliability of the enhanced ICA algorithm are enhanced.

2. Most of the mixed signals in the engineering are nonlinear mixed signals, and thus it is a challenge work for most ICA algorithms to separate the sources accurately. To overcome this challege, priori information is employed to weaken the uncertainty problem of nonlinear mixed signals. By the priori information, the separated signals can be better separated, and thus separating performance can be further enhanced, which can improve the accuracy of calculated contributions. Therefore, it provides another way to enhance the separating performance of ICA according to making full use of priori information.

6. Conclusions

As the influences of transmission paths, the vibration signals on the shell are influenced significantly, so it is a very challenging task to identify the sources and quantitatively evaluate the source contributions, which is important for vibration reduction and control.

In this paper, a novel method to quantitatively evaluate the source contributions based on the enhanced ICA algorithm and priori information is proposed. The enhanced ICA method provides a powerful way to effectively and reliably separate sources from the mixed signals. In the simulations, the comparative results show that principal component analysis cannot deal with some typical mechanical signals. Fast fixed point algorithm has strong separating performance for linear superstition signals, but the reliability is not very good because it is a statistical signal processing method. The enhanced ICA algorithm evaluates the separating components by clustering analysis and selects the optimal ICs as the best results. Therefore, the separating performance and reliability are significantly enhanced. The error of contributions calculated by the enhanced ICA algorithm is less than 4.8%, which indicates that the proposed method is of high accuracy.

The proposed method is applied to evaluate the source contributions of a thin shell structure. The priori information is discussed in two different separation process. The case that does not use priori information has an obvious error of 36.67%. Compared with the real values by measurement, the comparative results show that the proposed method obtains a high accuracy with priori information, and the relative error is less than 7.18%. Therefore, the proposed method can effectively evaluate source contributions, which can provide reliable referances for vibration reduction and monitoring.

7. Acknowledgement

8. References

Lee SK. Lee, Mace B.R., Brennan MJ. (2007). Wave propagation, reflection and transmission in curved beams. *Journal of Sound and Vibration*, vol.306, no.3-5: pp.636–656, ISSN: 0022-460X

Senjanovic. I, Tomasevic. S, Vladimir. N. (2009). An advanced theory of thin-walled girders with application to ship vibrations. *Marine Structures*, vol.22, no.3: pp.387–437, ISSN: 0951-8339

Niu. JC, Song. KJ, Lim .CW. (2005). On active vibration isolation of floating raft system. *Journal of Sound and Vibration*, vol.285, no.1-2: pp.391–406, ISSN: 0022-460X

Otrin. M, Boltezar. M. (2009). On the modeling of vibration transmission over a spatially curved cable with casing. *Journal of Sound and Vibration*, vol.325, no.4-5: pp.798–815, ISSN: 0022-460X

Lee. YY, Su. RKL, Ng. CF. (2009). The effect of modal energy transfer on the sound radiation and vibration of a curved panel theory and experiment. *Journal of sound and vibration*, vol.324, no.3-5: pp.1003-1015, ISSN: 0022-460X

Xie. SL, Or. SW, Chan. HLW. (2007). Analysis of vibration power flow from a vibrating machinery to a floating elastic panel. *Mechanical Systems and Signal Processing*, vol.21, no.1: pp.389–404, ISSN: 0888-3270

Bonfiglio. P, Pompoli. F, Peplow. AT. (2007). Aspects of computational vibration transmission for sandwich panels. *Journal of Sound and Vibration*, vol.303, no.3-5: pp.780–797, ISSN: 0022-460X

Efimtsov. BM, Lazarev. LA. (2009). Forced vibrations of plates and cylindrical shells with regular orthogonal system of stiffeners. *Journal of Sound and Vibration*, vol.327, no.1-2: pp.41–54, ISSN: 0022-460X

Li. XB. (2006). A new approach for free vibration analysis of thin circular cylindrical shell. *Journal of Sound and Vibration*, vol.296, no.1-2: pp.91-98, ISSN: 0022-460X

Cha. SL, Chun. HH. (2008). Insertion loss prediction of floating floors used in ship cabins. *Applied Acoustics*, vol.69, no.10: pp.913–917, ISSN: 0003-682X

Iijima. K, Yao. T, Moan. T. (2008). Structural response of a ship in severe seas considering global hydroelastic vibrations. *Marine Structures*, vol.21, no.4: pp.420–445, ISSN: 0951-8339

Tian RL, Pan. J, Peter. JO., et al. (2009). A study of vibration and vibration control of ship structures. *Marine Structures*, vol.22, no.4: pp.730-743, ISSN: 0951-8339

Jnifene. A. (2007). Active vibration control of flexible structures using delayed position feedback. *Systems & Control Letters*, vol.56, no.3: pp.215-222, ISSN: 0167-6911

Barrault. G, Halim. D, Hansen. C, et al. (2008). High frequency spatial vibration control for complex structures, *Applied Acoustic*, vol.69, no.11: pp.933-944, ISSN: 0003-682X

Jutten. C, Herault. J. (1991). Blind separation of sources. Part I: An adaptive algorithm based on neuromimatic architecture. *Signal Processing*, vol.24, no.1: pp.1-10, ISSN: 0165-1684

Comon. P. (1994). Independent component analysis, a new concept? *Signal Processing* , vol.36, no.3: pp.287-314, ISSN: 0165-1684

Hyvarinen. A, Oja. E. (1997). A fast fixed-point algorithm for independent component analysis. *Neural Computation*, vol.9, no.7 : pp.1486-1492, ISBN: 0-262-58168-X

Hyvarinen. A. (1999). Fast and robust fixed-point algorithm for independent component analysis. *IEEE Transactions On Neural Network*, vol.10, no.3 : pp.626-634, ISSN: 1045-9227

Hyvarinen. A, Karhunen. J, Oja. E. (2001). In : *Independent component analysis*. John Wiley and Sons. ISBN : 0-471-40540-X, New York, USA

Hu. HF. (2008). ICA-based neighborhood preserving analysis for face recognition. *Computer Vision and Image Understanding*, vol.112, no.3: pp.286-295, ISSN: 1077-3142

Correa. N, Adali. T, Vince. Calhoun. VD. (2007). Performance of blind source separation algorithms for fMRI analysis using a group ICA method. *Magnetic Resonance Imaging*, vol.25, no.5: 684–694, ISSN : 0730-725X

Ye. YL, Zhang. ZL, Zeng. JZ. (2008). A fast and adaptive ICA algorithm with its application to fetal electrocardiogram extraction. *Applied Mathematics and Computation*, vol.205, no.2: pp.799-806, ISSN : 0096-3003

Xie. L, Wu. J. (2006). Global optimal ICA and its application in MEG data analysis. *Neurocomputing*, vol.69, no.16-18: pp.2438-2442, ISSN: 0925-2312

Zuo. MJ, Lin. J, Fan. XF. (2005). Feature separation using ICA for a one-dimensional time series and its application in fault detection. *Journal of Sound and Vibration*, vol.287, no.3: pp.614-624, ISSN: 0022-460X

Moussaoui. S, Hauksdottir. H, Schmidt. F. (2008). On the decomposition of Mars hyper-spectral data by ICA and Bayesian positive source separation. *Neurocomputing*, vol.71, no10-12: pp.2194–2208, ISSN : 0925-2312

Kwak. N, Kim. C, Kim. H. (2008). Dimensionality reduction based on ICA for regression problems. *Neurocomputing*, vol.71, no.13-15: pp.2596– 2603, ISSN: 0925-2312

Himberg. J, Hyvarinen. A. (2003). Icasso: Software for investigating the reliability of ICA estimates by clustering and visualization. *IEEE XIII Workshops On Neural Networks for Signal Processing*, pp. 259-268, ISBN: 0-7803-8177-7, Toulouse, France

Himberg. J, Hyvarinen. A, Esposito. F. (2004). Validating the independent components of neuroimaging time-series via clustering and visualization. *Neuroimage*, vol.22, no.3: pp.1214-1222, ISSN: 1053-8119

Ma. JC, Niu. YL, Chen. HY. (2006). In : *Blind Signal Processing*. National Defense Industry Press, pp.150-160, ISBN: 9787118045079, BeiJing, China

He. ZJ, Zi. YY, Zhang. XN. (2006). In : *Modern signal processing technology and its application*, Xi'an Jiaotong University Press, pp.4-9, ISBN: 9787560525464, Xi'an, China
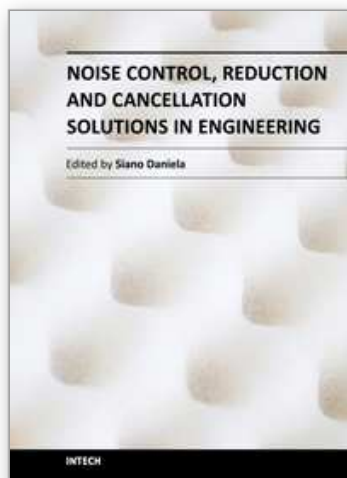
Noise Control, Reduction and Cancellation Solutions in Engineering

Edited by Dr Daniela Siano

Noise has various effects on comfort, performance, and human health. For this reason, noise control plays an increasingly central role in the development of modern industrial and engineering applications. Nowadays, the noise control problem excites and attracts the attention of a great number of scientists in different disciplines. Indeed, noise control has a wide variety of applications in manufacturing, industrial operations, and consumer products. The main purpose of this book, organized in 13 chapters, is to present a comprehensive overview of recent advances in noise control and its applications in different research fields. The authors provide a range of practical applications of current and past noise control strategies in different real engineering problems. It is well addressed to researchers and engineers who have specific knowledge in acoustic problems. I would like to thank all the authors who accepted my invitation and agreed to share their work and experiences.

How to reference

In order to correctly reference this scholarly work, feel free to copy and paste the following:

Wei Cheng, Zhousuo Zhang and Zhengjia He (2012). Vibration Source Contribution Evaluation of a Thin Shell Structure Based on ICA, Noise Control, Reduction and Cancellation Solutions in Engineering, Dr Daniela Siano (Ed.), ISBN: 978-953-307-918-9, InTech, Available from: http://www.intechopen.com/books/noise-control-reduction-and-cancellation-solutions-in-engineering/-vibration-source-contribution-evaluation-of-a-thin-shell-structure-based-on-ica-not-the-source-cont

INTECH
open science | open minds